On the Feasibility of Coordinates-Based Resource Allocation Through Machine Learning

Sahar Imtiaz
Division of ISE, EECS School
KTH Royal Institute of Technology
Stockholm, Sweden
sahari@kth.se

Georgios P. Koudouridis
RAN System Lab, SRC
Huawei Technologies Sweden AB
Kista, Stockholm, Sweden
george.koudouridis@huawei.com

James Gross
Division of ISE, EECS School
KTH Royal Institute of Technology
Stockholm, Sweden
james.gross@ee.kth.se

***Abstract*—Over the last decade there has been a large research interest in exploiting terminal positions for various cellular network services and communication aspects. However, the relevance of terminal coordinates for resource allocation is relatively unexplored to date. In this work, we thus take a first step in that direction by studying coordinates-based resource allocation in an arguably favorable, and straightforward set-up. In particular, we consider the usage of supervised machine learning for resource allocation. Our results show that for the studied scenario, coordinates-based resource allocation can achieve a comparable performance to a CSI-based comparison scheme. While the main limiting factors are channel uncertainty as well as the accuracy of the terminal coordinates, in particular more complex machine learning schemes like Random Forests are able to provide some robustness despite the above mentioned noisy features.**

***Index Terms*—Wireless communication system, position coordinates, machine learning, resource allocation**

I. Introduction

Over the last two decades, the utilization of position information in wireless communication networks has been an intense research field [1], [2]. For instance, position information is fundamental for realizing location-based services [2], which is heavily leveraged for commercial services today. Furthermore, with respect to protocol stack optimization, position-based concepts have been proposed regarding security and privacy, routing, as well as relay selection [2]. For all these works, the accurate acquisition of the terminal position is vital. Correspondingly, localization has been a further intense research topic over the last two decades. Well-known approaches either rely on separate systems to obtain position information, such as global positioning system (GPS) or global navigation satellite systems (GNSS) [2], while alternatively the localization of a terminal can also be performed directly through the wireless communication system itself [3].

In contrast to the rather prominent research avenues above, only few works have considered usage of the position information of a terminal directly for resource allocation [4]. For instance, position-related information (i.e. angle-of-arrival) of mobile terminals is utilized in [3] for spatial filtering in an ultra-dense network to maximize throughput. Somewhat similar, the authors in [5] propose location-aided beamforming based on exploiting the distance between the base station and the mobile relay for beam selection to serve high-speed users. In [6], mobile terminal positions are predicted based on received signal strength samples. These predictions are then used to group transmit beams for resource allocation in millimeter-wave systems, where a reduction of the handover frequency is a side constraint. Finally, the work in [7] proposes to determine adaptive modulation and coding (AMC) decisions based on localization through fingerprinting. Interestingly, to the best of our knowledge, none of these previous works have considered resource allocation solely based on position coordinates of the mobile terminal. Furthermore, most of the above studies do not account for stochastic variations that position-related information typically is subject to. Thus, the basic question regarding the feasibility of a coordinates-based resource allocation scheme is open to date.

In this work, we attempt to make a first contribution towards this open direction. We ask which efficiency a coordinates-based resource allocation scheme can achieve in an arguably favorable and straightforward set-up. Towards this end, we assume an individual base station-terminal association in an urban-area, noise-limited, strong line-of-sight (LoS) scenario with multiple antennas and significant frequency diversity. In this setting, we consider the optimization of the downlink communication where the allocated resources comprise the transmit beam, receive filter and AMC setting. To determine appropriate allocations, the scheduling unit is only provided either accurate or noisy terminal coordinates. In this setting, we show that the application of supervised machine learning, in particular of Random Forests [8], has the potential for being an efficient and promising approach to resource allocation. Supervised machine learning is not new to resource allocation in wireless systems, however, previous works [9]–[11] have only considered the application to AMC decision solely. The major finding of our work is that the proposed approach performs surprisingly well when benchmarked against an upper bound, despite somewhat inaccurate positions availability and channel uncertainties. We acknowledge that the choice of channel model is key for the credibility of our study. We thus resort in all our investigations to the state-of-the-art ray tracing-based METIS channel model [12] used in standardization, which provides a high degree of realism.

The rest of this paper is structured as follows: Section II describes the system model. Section III focuses on the design

of the proposed approach, i.e. coordinates-based resource allocation through ML. Section IV presents the evaluation methodology, the results and relevant discussions. Finally, Section V concludes the paper.

II. System Model

We focus on the downlink communication between a single transmitter (i.e. base station, BS) and a single, mobile terminal. We assume the system to be operating on time frames of duration T_{f} [ms]. For payload transmission, we assume that the BS is equipped with A_{r} antennas operated collectively with a constant transmit power P_{Tx} [W]. The user terminal is assumed to have A_{n} receive antennas. The BS utilizes a system bandwidth W [Hz] with OFDM waveform assumed for transmission. Therefore, bandwidth W spans a number of sub-carriers N with the center frequency denoted by f_{c} [Hz].

The wireless communication channel between the BS and the terminal is assumed to be a time-varying communication channel subject to path loss, shadowing and fading. We denote the MIMO channel matrix representing the channel states from all transmit to receive antennas at time point t and for sub-carrier n by $\boldsymbol{H}(t,n)$. Moreover, we assume that the MIMO channel stays constant within the duration of a single frame, and that the user terminal is not exposed to any interference. If the BS applies transmit beam $\boldsymbol{v}$ at time t to transmit the symbol $s(t,n)$ over sub-carrier n, while the terminal applies filter $\boldsymbol{u}$, the received downlink signal is given as:

$$y(t,n) = \sqrt{P_{\mathrm{Tx}}} \cdot (\boldsymbol{u}(t))^{\dagger} \cdot \boldsymbol{H}(t,n) \cdot \boldsymbol{v}(t) \cdot s(t,n) + \boldsymbol{z}, \quad (1)$$

where $\boldsymbol{z}$ represents additive white Gaussian noise, while $(\boldsymbol{u}(t))^{\dagger}$ represents the Hermitian of $\boldsymbol{u}(t)$. Thus, the signal-to-noise ratio (SNR) for the terminal served by the BS at time t for sub-carrier n, with noise power ${\sigma_z}^2$, is given by:

$$\gamma(t,n) = \frac{P_{\mathrm{Tx}} \cdot |(\boldsymbol{u}(t))^{\dagger} \cdot \boldsymbol{H}(t,n) \cdot \boldsymbol{v}(t)|^2}{{\sigma_z}^2}. \quad (2)$$

A. Resource Allocation

Before payload transmission, the BS determines a resource allocation. In this paper, a resource allocation $\mathfrak{r}(t)$ is given by (a) a choice of transmit beam $\boldsymbol{v}(t)$ for the BS-terminal pair, chosen from the finite set $\mathbb{V}$ of available beams; (b) a choice of receive filter $\boldsymbol{u}(t)$ for the terminal, chosen from the finite set $\mathbb{U}$ of available filters; and finally (c) a choice of modulation and coding scheme (MCS) $\mathfrak{m}(t)$, chosen from the finite set $\mathbb{M}$ of available MCSs. Note that we assume a uniform application of the chosen MCS over all sub-carriers N, i.e. the system does not feature adaptive MCS per sub-carrier.

We assume full-buffer state at the BS with respect to the terminal. Hence, for the chosen MCS, the subsequent payload data transmission carries the maximum amount of possible bits, denoted by function $b(\mathfrak{m}(t))$. Due to noise, this data transmission can be received erroneously, with the event likelihood represented by a link-to-system model $e(\mathfrak{m}(t), \gamma_{\mathrm{eff}}(t))$ described in [13]. Here, $\gamma_{\mathrm{eff}}(t)$ is effective SNR over all sub-carriers. We rely on the exponential effective SNR mapping, which converts the SNR value $\gamma(t,n)$ per sub-carrier into an equivalent SNR regarding the entire transmission system. Hence, the link-to-system model $e(\cdot)$ represents the relationship of block error rate, effective SNR, MCS as well as payload size. This results in the transport capacity $\mathcal{T}(t)$ (i.e goodput) for the terminal, given by:

$$\mathcal{T}(t) = [1 - e(\mathfrak{m}(t), \gamma_{\mathrm{eff}}(t))] \cdot b(\mathfrak{m}(t)). \quad (3)$$

Based on this model, per downlink frame, the following optimization problem is now of interest (skipping index t):

$$\max_{\boldsymbol{v},\boldsymbol{u},\mathfrak{m}} \mathcal{T} = [1 - e(\mathfrak{m}, \gamma_{\mathrm{eff}})] \cdot b(\mathfrak{m}) \quad (4)$$
$$\text{s.t.} \quad \gamma_{\mathrm{eff}} \geq \gamma_{\min} > 0,$$
$$\mathfrak{m} \in \mathbb{M}; \boldsymbol{u} \in \mathbb{U}; \boldsymbol{v} \in \mathbb{V}.$$

The first constraint assures that the effective SNR for the BS-terminal pair is above a certain threshold $\gamma_{\min}$ to ensure a decodable signal. The principle amount of feasible solutions for the optimization problem is given by $2 \cdot |\mathbb{V}| \cdot |\mathbb{U}| \cdot |\mathbb{M}|$. The above problem is a combinatorial, non-linear optimization problem due to the (non-linear) channel effects existing in the propagation environment. Therefore, heuristic approaches have been proposed in the literature [14]. Note that such heuristics rely on channel state information (CSI) available at the BS.

B. Problem Statement

We denote the position coordinates of the terminal at time t by $\boldsymbol{p}(t)$, whereas $\hat{\boldsymbol{p}}(t)$ denotes an estimate of the terminal's position available at the BS. This position estimate $\hat{\boldsymbol{p}}(t)$ can, for example, be determined by extended Kalman filtering of the direction-of-arrival (DoA) and time-of-arrival (ToA) of specifically sent positioning beacons [3]. However, the modeling of this piloting phase is out of the scope of this paper. Instead, we only consider a potential position estimation error $(\boldsymbol{p}(t) - \hat{\boldsymbol{p}}(t))$, which we model as a Gaussian zero-mean random variable with variance σ^2 that depends on the accurate estimation of DoA and ToA parameters; the former depends on the antennas' geometry, the latter on the path loss.

Instead of following the default assumption of CSI being available at the BS, we propose instead to allocate resources $\mathfrak{r}(t)$ by a trained model through supervised ML. For this process, the terminal position estimate $\hat{\boldsymbol{p}}(t)$ serves as input to the trained model, while the resource allocation decision is supposed to solve the capacity maximization problem (4). In other words, we are interested in determining how valuable the position estimates are for resource allocation, whether supervised ML can provide a suitable resource allocation model, and under which conditions this approach is viable.

III. Coordinates-Based Resource Allocation Through Machine Learning

We consider different operation modes for the assumed system. During the *data-collection mode*, the system operates in legacy CSI-based allocation mode. However, it simultaneously collects also the user position estimates $\hat{\boldsymbol{p}}(t)$ over an extended period of time. After the collection of a sizeable amount of position estimates, as well as their channel states, optimal

resource allocations $\mathfrak{r}(t)$ are determined offline for each sample. This is performed by exhaustive search in order to solve Problem (4). The combination of position estimate $\hat{\boldsymbol{p}}_i(t)$ and optimal resource allocation $\mathfrak{r}_i(t)$ constitutes a *training sample* i with the position estimate being the input parameter - also referred to as feature $\boldsymbol{x}$ - while the resource allocation is the output - also referred to as class. The entirety of collected and processed training samples is referred to as training dataset $\boldsymbol{D}$. From this training dataset $\boldsymbol{D}$, the corresponding resource allocation model is generated (offline) by ML. Once such resource allocation model is available, the system switches to the *position-based mode*. Now, for each time frame (and hence for each resource allocation) the current position estimate of the terminal is passed to the model, which generates (predicts) a matching resource allocation.

For model generation, we consider two well-known supervised ML algorithms, namely K-nearest neighbor (KNN) and Random Forests (RF). KNN is the simplest ML classifier, whereas RF is a more complex supervised ML algorithm. The choice of RF is motivated by the inherent noisiness of the position estimates, since RF is known to have some degree of robustness to noisy features. Due to low-dimensional input data, training a deep neural network is not considered.

A. K-Nearest Neighbor

KNN is a straightforward ML classifier [15], which does not build a learning model explicitly. Instead, it generates predictions directly from the training data. In the context of coordinates-based resource allocation, for any given position estimate KNN finds its K nearest neighbors (i.e. the K closest positions) from all features of the training data $\boldsymbol{D}$. The predicted resource allocation for this given position estimate results then from a majority vote over all respective K classes. Thus, in case of a suitably dense position sampling in the training data set, one can expect KNN to accurately identify any spatial dependencies of the resource allocations.

B. Random Forests

In contrast to KNN, RF [8] is more involved. It basically consists of a distinct data structure for the trained model, as well as an algorithm to parameterize this data structure from the training data. As the name suggests, RF utilizes multiple random binary decision trees, making up a *forest*, as data structure for the trained model. Specifically, Ω_t binary random trees are utilized, each with a maximum depth Ω_d. For each tree, the root node as well as the interior nodes are populated with decision thresholds, while each leaf node stores a corresponding class (resource allocation). The training algorithm first formulates a data set of the same size as $\boldsymbol{D}$ by bootstrap sampling (i.e. sampling with replacement) from the training data set $\boldsymbol{D}$. Then it constructs a decision tree with the bootstrapped samples, where the decision thresholds at the root node as well as the interior nodes are formed on randomly selected number of features, given by floor($\sqrt{\text{number of features } \boldsymbol{x}}$). The interior nodes keep on growing in the tree until either all the classes are perfectly classified, or the level of the interior nodes reaches Ω_d. This algorithm is then repeated Ω_t times to form a trained model of the RF. In terms of the coordinates-based resource allocation scheme, whenever a new position estimate (feature $\boldsymbol{x}$) is available, it is parsed through all the trees in the trained forest to collect Ω_t classes. The resource allocation is then determined by majority vote, i.e. bootstrap aggregating [8].

The bootstrap aggregation in RF provides some degree of robustness, particularly for noisy classes. In addition, the formulation of decision thresholds for each of the tree nodes using randomly selected number of features for bootstrapped samples makes the trees uncorrelated, which improves the prediction accuracy of RF compared to simpler classification ML algorithms, such as KNN.

IV. Performance Evaluation and Discussion

In this paper, we are essentially interested in the viability of a coordinates-based resource allocation scheme. Towards this end, we benchmark different approaches to highlight (a) the efficiency of any coordinates-based approach in comparison to a traditional CSI-based scheme; (b) the efficiency of supervised machine-learning in comparison to an alternative coordinates-based scheme; (c) the impact of different random effects on all coordinates-based resource allocation schemes. Our general evaluation means is by computer simulations, while the principle performance metric is the objective function in (4), i.e. the transport capacity. We emphasize in particular the importance of the accuracy of the chosen models (as well as their implementations) of the computer simulations as key factor for the credibility of our results. In the following, we therefore provide first more details on the general scenario and methodology, as well as the details of the channel model, before we present the results of our evaluation.

A. Scenario Choice and Evaluation Methodology

We generally consider an urban-area setting of a future mobile communication system. Specifically, the simulation scenario comprises a street section of 6×25 m^2, where the BS is placed 3 m away from the street along the x-axis. The system bandwidth W is set to 200 MHz, with the operational center frequency f_c of 3.5 GHz. The BS is equipped with $A_\mathrm{r} = \{8, 4\}$ antennas, each at a height of 10 m from the ground. The user terminal has $A_\mathrm{n} = \{1, 2\}$ antenna elements, with a height of 1.5 m from the ground. The BS operates the antennas with a constant power P_Tx of 1μW per antenna, while the transmission time interval of the system is set to $T_\mathrm{f} = 0.2$ ms. Both the BS and the user terminal antenna elements are Hertzian dipoles, placed to form linear arrays oriented along the x-axis. In terms of system resources for the different resource allocation (RA) schemes, a fixed set of transmit beams and receive filters is generated based on an angular separation of θ°. The MCS set corresponds to LTE, with 15 different values, where the effective SNR ranges applied for different MCS are taken from [16]. However, the MCS value chosen for resource allocation is determined by optimally solving the Problem (4).

The different comparison schemes are defined as follows:

- **Genie:** This scheme serves as the upper bound for evaluation. It represents the optimal solution to Problem (4) given perfect CSI.
- **Geometric-based RA Scheme:** This coordinates-based scheme serves as a benchmark for the two ML-based schemes. We consider for this geometric beamforming, i.e. the transmit beam and the receive filter are allocated based on the geometry of the user's position estimate in relation to the BS. In addition, the MCS is determined statistically based on the terminal position as well.
- **KNN-based RA Scheme:** As discussed in Section III-A. In particular, we set $K = 1$ for all our evaluations as a result of initial testing.
- **RF-based RA Scheme:** As discussed in Section III-B. In terms of parameterization, we set $\Omega_t = 100$ trees with a maximum depth of $\Omega_d = 15$ for all our evaluations, again as a result of initial testing.

In order to address the goals of our performance study, we consider the following three main parameter variations:

- **Antenna Configurations:** We consider set-ups with 8×1, 8×2 and 4×2 antennas on BS and terminal side. The rational behind these choices is to study the impact of the dimensionality of the optimization problem (4) as well as of the spatial selectivity of the terminal on the considered approaches. For the first two configurations ($A_\mathrm{r} = 8$), we consider $\theta = 3°$ for the transmit beamforming vectors, therefore, $|\mathbb{V}| = 58$. For A_r = 4, the angular separation gets doubled, i.e. $\theta = 6°$, and hence, $|\mathbb{V}| = 29$. For receive filter with $A_\mathrm{n} = 2$, we consider $\theta = 12°$, thus $|\mathbb{U}| = 16$.
- **Scatterers' Density:** The exact channel generation method is discussed further below. However, the scatterers' density ρ, and subsequently the random placement of scatterers according to the chosen density, is a key parameter which determines the randomness of the considered channel model. We vary the scatterers' density in the following by setting $\rho = 0$, 0.01 and 0.05/m^2, which results into at most 0, 1 or 5 reflecting objects (such as cars) on the considered street section[1].
- **Position Estimate Error:** A further key parameter impacting all coordinates-based schemes is the accuracy of the position estimate. We vary this accuracy by setting $\sigma = 0$, 0.25, 0.4 and 1 m.

Given a chosen system set-up, the general procedure for an evaluation is as follows. We initially generate random terminal positions and determine from them matching channel matrices (see next subsection for the channel generation method). We ignore detailed terminal mobility models, and simply perform uniformly distributed terminal drops. Note that due to the chosen propagation scenario, and geometric set-up of the antennas, all considered drops belong to a LoS scenario. We then form the training data by determining the optimal resource allocations, followed by training of the ML algorithm. Given the trained resource allocation model, we apply the different approaches discussed earlier for resource allocation. For all considered evaluations, we generate a total of 125,000 position drops, resulting in a similar amount of training samples. Two-thirds of the samples are generally used for training while the rest are used for evaluations.

Finally, a subtle detail relates to the representation of the training data before being processed by the ML algorithm. Each feature (i.e. terminal position) of the data set is represented as $\boldsymbol{x}_i$. Furthermore, each class $\mathfrak{r}_i(t)$ (i.e. resource allocation) of training sample i is basically represented in the binary sequence ($\boldsymbol{v}, \boldsymbol{u}, \mathfrak{m}$, corresponding to always first representing the index of the transmit beam, then the index of receive filter and finally the MCS index). Nevertheless, in particular due to the dimensionality of the classes resulting from the total number of combinations, this approach leads to long bit strings which are sparse. Thus, after obtaining all classes for a given data set, we re-index the classes by bit strings that match exactly the cardinality of the set of occurred classes (versus the set of potential classes). This is an important reduction of the solution space.

B. Channel Generation

As already mentioned, a key factor of our study is a realistic channel generation. For this we resort to the ray-tracing based METIS channel model for the Madrid grid [12], which is one of the most realistic channel models available for simulations, and has been validated for different propagation scenarios. For downlink communication with a single BS and a single user terminal, the ray-tracing model determines k multipath components for each time t and frequency n resource. These multipath components are the result of different waveform transmission phenomena, including reflection, diffraction and scattering, which are affected by the presence of scatterers, such as cars, in the propagation environment. The ray-tracing model also takes into account the radiation pattern of antennas for both the BS and the user terminal. Let $\tilde{h}_{k,a_\mathrm{n},a_\mathrm{r}}(t,f)$ denote the impulse response for multipath component k, between each BS antenna element a_r and user terminal's antenna element a_n, which captures all the aforementioned effects of the propagation environment, as well as the relevant pathloss. The channel impulse response is then the sum of the impulse responses $\tilde{h}_{k,a_\mathrm{n},a_\mathrm{r}}(t,n)$ from k different multipath components, given by:

$$H_{a_\mathrm{n},a_\mathrm{r}}(t,n) = \sum_{k=1}^{K} \tilde{h}_{k,a_\mathrm{n},a_\mathrm{r}}(t,n) \cdot \cdot e^{\frac{j2\pi d_k(t)}{\lambda}} e^{-j2\pi f_n \tau_{k,a_\mathrm{r},a_\mathrm{n}}(t)}. \quad (5)$$

Here, $H_{a_\mathrm{n},a_\mathrm{r}}(t,n)$ denotes the element of $\boldsymbol{H}(t,n)$ that corresponds to the complex polarimetric channel impulse response between each a_r and a_n. K is the total number of multipath components, λ is the wavelength, f_n is the frequency of subcarrrier n and d_k is the total distance for multipath k at time t.

[1]The channel generator actually uses the scatterer density ρ to randomly place scatterers *up to* a number that corresponds to ρ. For example, in the case of ρ = 0.05/m^2, up to 5 scatterers are present and placed arbitrarily in the simulation environment.

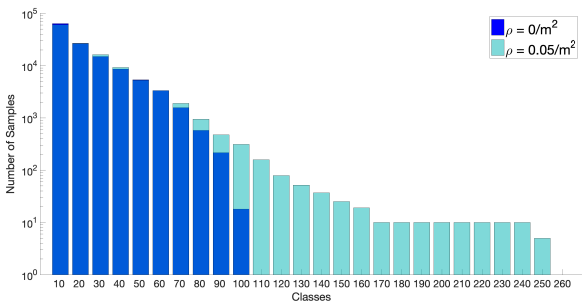

Fig. 1. Distribution of the number of samples per class, for (a) ρ = 0/m^2, and (b) ρ = 0.05/m^2, for 8 × 2 MIMO system.

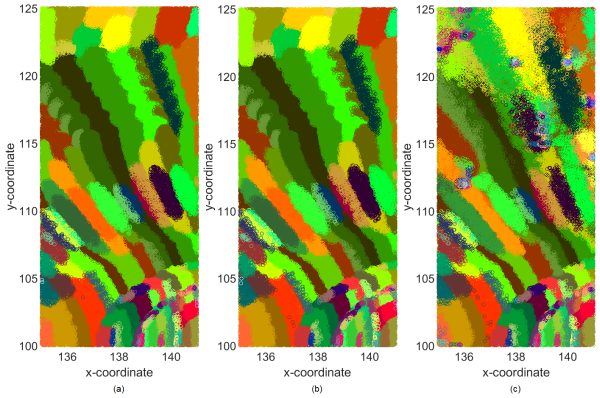

Fig. 2. Class distribution for different user positions with 8×2 MIMO system for (a) ρ = 0/m^2, (b) ρ = 0.01/m^2, and (c) ρ = 0.05/m^2.

τ_{k,a_n,a_r} denotes the delay for path k. A detailed implementation for the channel model can be found in [3].

C. Initial Analysis of the Dataset

We start with a general characterization of the generated training data sets for a base case, with the specific parameters ρ = 0, 0.01, 0.05/m^2, σ = 0 m, $A_r \times A_n$ = 8×2, and θ = 3°, 12° for $\mathbb{V}$ and $\mathbb{U}$, respectively. Thus, we analyse the data set for ground truth regarding the positions while varying the amount of scatterers (up to 0, 1, or 5 scatterers). Note that for a scatterer density of 0/m^2 the considered channel generation is deterministic, i.e. the channel between a given terminal position and BS is always resulting in the same channel $\boldsymbol{H}(t, n)$.

Figure 1 shows the resulting class distribution of the training data sets. We only represent here the cases of ρ = 0/m^2 and 0.05/m^2. Note in the figure that the x-axis is batched in groups of ten classes for illustration purposes. In general, we observe an exponential distribution for the number of samples per class. The number of classes for ρ = 0.05/m^2 (254) is almost 3× the one for ρ = 0/m^2 (94). However, in both cases, the total number of classes is rather low compared to the total size of the data set (125,000 samples). More scatterers imply more multipath components, which vary with scatterers' placement, introducing more randomness in the channel. This means that for a fixed user position with different placement of the scatterers, the channel response varies, resulting in different optimal resource allocations.

Figure 2 shows the distribution of classes for the considered user positions, for a maximum scatterer density ρ of 0, 0.01, 0.05/m^2. To be more precise, the plots show the spatial clustering of classes (i.e. resource allocations) where each class is represented by a unique color. From Figure 2, we see that the class boundaries are quite distinct in all of the plots. For the areas further away from the BS (note that the BS is positioned in the lower right corner of the plots), larger spatial clusters exist. In contrast, the spatial clusters become much smaller in particular close to the BS. Note that different colors of neighboring clusters potentially can be due to any difference in the resource allocation (i.e. either only a slightly different choice in transmit beam, for example, up to a totally different choice in all three class components). The plot for

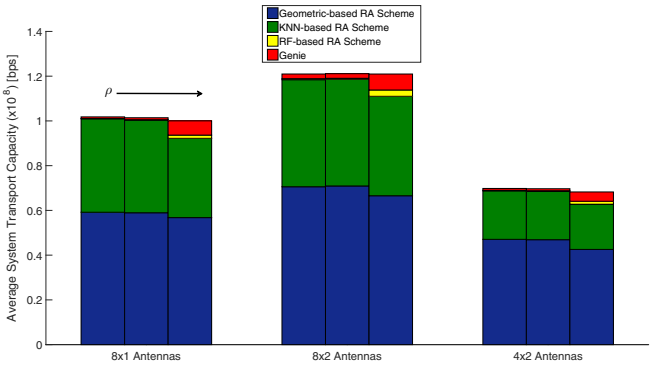

Fig. 3. Average transport capacity for different antenna configurations with accurate position estimates. The density of scatterers increases from left to right (0/m^2, 0.01/m^2 and 0.05/m^2) within a group of bar plots.

ρ = 0.05/m^2 shows the impact of the random placement of scatterers. Here, certain class clusters become 'blurred' due to scatterer placements leading to strictly different classes for close-by drops. This already hints to a potential challenge for coordinates-based resource allocation schemes.

Overall, we conclude from Figure 2 a strong spatial clustering, which suggests the feasibility of a coordinates-based resource allocation scheme. The relatively low number of classes, as represented in Figure 1, supports this conclusion. However, Figure 2 also reveals the challenges for such a scheme. Most importantly, the class clusters are not necessarily evenly oriented in a geometric sense, which immediately points to the use of ML. Furthermore, erroneous positions will pose a challenge due to the unevenly distributed clusters.

D. Results and Discussion

We now move on to the discussion of the different resource allocation schemes in different scenarios. We start with the presentation of the performance results in case of varying the antenna configurations and the scatterers' density, while providing *perfect position information* at the BS. Figure 3 shows the resulting average transport capacity. The bar plots are grouped along the antenna configurations, and per group

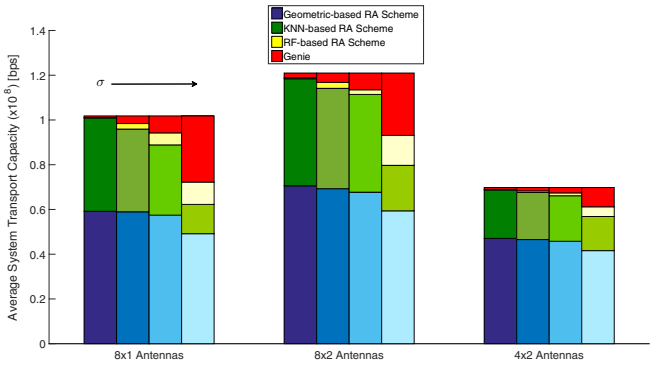

Fig. 4. Average transport capacity for assumed system for different position inaccuracies, with ρ = 0/m^2, for different antenna configurations.

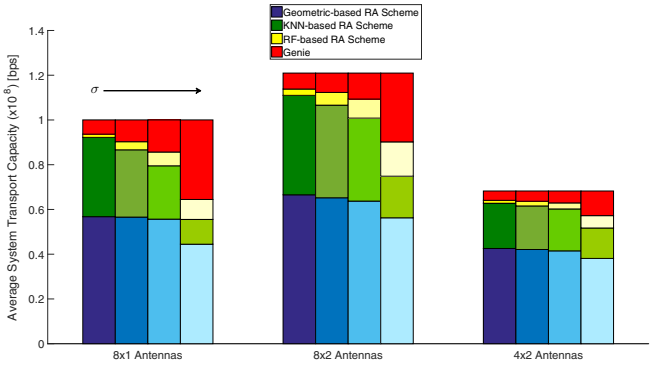

Fig. 5. Average transport capacity for assumed system for different position inaccuracies, with ρ = 0.05/m^2, for different antenna configurations.

we increase the amount of maximum scatterers from left to right. As expected, the antenna configuration 8×2 provides the highest overall performance, whereas the other two schemes have significantly lower performance (4×2 has 50% of 8×2, whereas 8×1 has 75% of 8×2). Moreover, both the coordinates-based KNN- and RF-based schemes show performance results very close to the genie when $\rho = 0/\text{m}^2$, for all antenna configurations. This gap remains small even in the case of $\rho = 0.01/\text{m}^2$ while it widens to about 10% in case of $\rho = 0.05/\text{m}^2$. For $\rho = 0.05/\text{m}^2$, the RF-based RA scheme performs slightly better than the KNN-based RA scheme, otherwise the two schemes are more or less identical. In contrast, the geometric-based RA scheme performs the worst, around 50% of the genie performance, for antenna configurations of 8×1 and 8×2 (59.2 Mpbs vs 101.8 Mbps, and 70.6 Mpbs vs 120.96 Mbps, respectively), while for 4×2 the performance gap is significantly less.

Even though these results relate to a hypothetical case with perfect position information, they reveal already several conclusions. First, as Section IV-C already indicated, coordinates-based resource allocation appears to have a significant potential. The spatial structure of optimal resource allocations, at least in the considered model, can be efficiently exploited for resource allocation using ML. This potential is not significantly diminished by the choice of the multi-antenna system. However, generally speaking, the higher the directivity of the multi-antenna system is, the more important is the consideration of the uneven spatial clustering, which appears to be only captured efficiently by ML models, but not by geometrically driven approaches. Finally, the differences between the two ML-driven schemes are mostly marginal.

We next turn to the more realistic cases with erroneous position information at the BS. In Figure 4 we present results for all antenna configurations with respect to the degrading position accuracy while setting the scatterer density to $\rho = 0/\text{m}^2$. Per antenna configuration, the different bar plots stand for an increasing error variance on the position information (from left to right). Furthermore, in Figure 5 we show the same results, however, setting the scatterers' density now to the highest value of $\rho = 0.05/\text{m}^2$. Thus, Figure 4 stands for a deterministic channel with gradually worsening position information, while Figure 5 stands for a (mildly) random channel behavior for the same gradual decay of the position information accuracy.

From Figures 4 and 5, we first of all observe the same absolute performance variations with respect to the different antenna configurations as before: 8×2 has the highest overall performance while the other two combinations have smaller absolute capacities. However, as the position information becomes now erroneous, the different coordinates-based schemes are impacted in different ways. Let us first consider the case with no scatterers in Figure 4. As the position information becomes erroneous, all three coordinates-based schemes are subject to an increasing performance degradation. This degradation effect can be mitigated the best by RF, which is clearly due to it's inherent robustness to noisy features. Unless the position inaccuracy is very strong, RF is within 90% of the maximal performance (i.e the genie), which also holds for Figure 5 with a large number of scatterers. In contrast, KNN typically stays within 80% of the maximal performance, while the geometric-based approach achieves typically a performance of around 50% and less of the maximal performance.

Thus, the major conclusions from Figures 4 and 5 are as follows: First of all, erroneous position information does not significantly diminish the performance of coordinates-based resource allocation based on ML. While Figure 2 might have given room for the hypothesis that erroneous position information leads to frequent misclassifications, even if this is happening, they do not appear to be significant with respect to the performance impact. Second, coordinates-based resource allocation based on ML is more vulnerable to erroneous position information than the geometric-based approach (which has a remarkably stable performance unless the position information is strongly erroneous). Finally, more sophisticated learning schemes like RF pay off in terms of robustness against position inaccuracies and mild channel uncertainties. This performance advantage is perhaps less than what could have been expected, but it is significant enough to spend the corresponding complexity (in comparison to KNN).

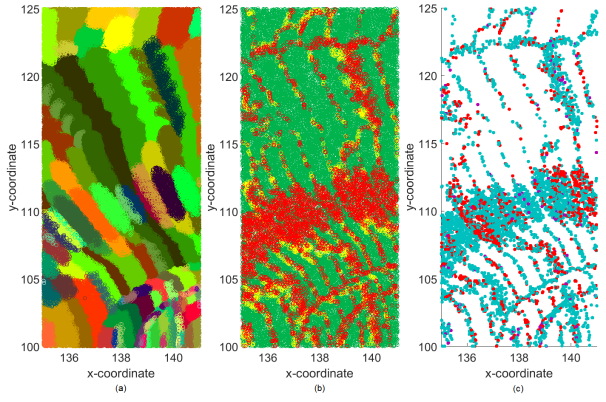

Fig. 6. Class distribution plots with σ = 0 m, ρ = 0/m^2 for (a) the original dataset, (b) the system performance as predicted by the RF algorithm, and (c) the performance-loss margin for lossy misclassification.

Can the performance of RF be improved in general? In order to clarify this question, we finally present an analysis of the misclassifications of the RF under perfect position information and deterministic channel conditions (i.e. no scatterers). We hypothesize that this set-up is the best one to study the possibly inherent misclassifications happening in RF due to its randomized learning approach in building the trees. In Figure 6(a) we show the basic plot of the clustered classes in this case (which corresponds to Figure 2) as well as two representations of the classification performance of RF on top of this ground truth. Figure 6(b) shows in green the correctly classified resource allocations, whereas yellow and red represent the misclassifications. We illustrate in yellow the misclassifications that do not have a performance impact, while red ones do. These red misclassifications are further quantified in Figure 6(c), where blue-colored samples show a performance loss of less than 10%, the purple-colored samples have a loss between 10-30%, and red-colored samples have a performance loss of more than 30%. Considering especially Figure 6(c) that relates to the significant misclassifications, we observe that these generally happen at the boundaries of class clusters (which is virtually happening throughout the entire area, albeit these misclassifications are rather mild). On the other hand, there is a 'band of misclassifications' in the middle of the considered scenario, where significant misclassifications are concentrated. This happens because the learning model becomes more conservative in allocating a higher MCS value for a given user position estimate. It is open to date how to address this issue, while these misclassifications incur a significant performance loss in the performance evaluations. The fact that there are systematic misclassifications hints probably to some existing remedy, which we nevertheless still need to explore.

V. Conclusion

This paper presents the idea of performing resource allocation based solely on the position coordinates of the mobile terminal through ML. The performance of the coordinates-based resource allocation scheme is benchmarked against a CSI-based genie as well as a geometric-based scheme. Our results show that the coordinates-based resource allocation scheme using ML has the potential to perform resource allocations more or less on par with the CSI-based scheme. This performance potential is retained by the proposed scheme unless the available position estimates become extremely erroneous. As future work we are interested in further improvements for the given straightforward set-up, as well as considering multi-terminal scenarios.

Acknowledgment

Major parts of this work were accomplished by utilizing resources provided by the Swedish National Infrastructure for Computing (SNIC) at PDC, KTH.

References

[1] Y. . Ko and N. H. Vaidya, "Geocasting in Mobile Ad Hoc Networks: Location-based Multicast Algorithms," in *Proceedings of 2nd IEEE WMCSA*, Feb 1999, pp. 101–110.

[2] R. Di Taranto *et al.*, "Location-Aware Communications for 5G Networks: How Location Information can Improve Scalability, Latency, and Robustness of 5G," *IEEE Signal Processing Magazine*, vol. 31, no. 6, pp. 102–112, Nov 2014.

[3] P. Kela *et al.*, "Location Based Beamforming in 5G Ultra-Dense Networks," in *2016 IEEE 84th Vehicular Technology Conference (VTC-Fall)*, Sept 2016, pp. 1–7.

[4] D. Slock, "Location Aided Wireless Communications," in *5th International Symposium on Communications, Control and Signal Processing*, May 2012, pp. 1–6.

[5] X. Chen, J. Lu, P. Fan, and K. B. Letaief, "Massive MIMO Beamforming With Transmit Diversity for High Mobility Wireless Communications," *IEEE Access*, vol. 5, pp. 23 032–23 045, 2017.

[6] S. H. Cha, J. S. Kim, and M. Y. Chung, "Coordinated-Beam Selection Scheme Using Mobility Pattern of Mobile Device in 5G Mobile Communication Systems," in *Proceedings of the 11th International Conference on Ubiquitous Information Management and Communication*, ser. IMCOM '17. New York, NY, USA: ACM, 2017, pp. 53:1–53:6.

[7] S. Sand, R. Tanbourgi, C. Mensing, and R. Raulefs, "Position Aware Adaptive Communication Systems," in *43rd Asilomar Conference on Signals, Systems and Computers*, Nov 2009, pp. 73–77.

[8] L. Breiman, "Random Forests," *Machine Learning*, vol. 45, no. 1, pp. 5–32, 2001.

[9] J. Cui, Z. Ding, and P. Fan, "The Application of Machine Learning in mmWave-NOMA Systems," in *87th IEEE VTC*, June 2018, pp. 1–6.

[10] J. P. Leite, P. H. P. de Carvalho, and R. D. Vieira, "A Flexible Framework Based on Reinforcement Learning for Adaptive Modulation and Coding in OFDM Wireless Systems," in *IEEE WCNC*, April 2012, pp. 809–814.

[11] S. Imtiaz, H. Ghauch, G. P. Koudouridis, and J. Gross, "Random Forests Resource Allocation for 5G Systems: Performance and Robustness Study," in *IEEE WCNC Workshops*, April 2018, pp. 326–331.

[12] V. Nurmela *et al.*, "Deliverable D1. 4 METIS Channel Models," in *Proc. Mobile Wireless Communication Enablers Inf. Soc.(METIS)*, 2015.

[13] E. Tuomaala and H. Wang, "Effective SINR Approach of Link to System Mapping in OFDM/Multi-Carrier Mobile Network," in *2nd Asia Pacific Conference on Mobile Technology, Applications and Systems*, Nov 2005.

[14] Y. Arikawa, H. Uzawa, T. Sakamoto, and S. Shigematsu, "High-Speed Radio-Resource Scheduling for 5G Ultra-High-Density Distributed Antenna Systems," in *8th International Conference on Wireless Communications Signal Processing*, Oct 2016, pp. 1–5.

[15] R. O. Duda, P. E. Hart, and D. G. Stork, "Pattern Classification and Scene Analysis," *2nd ed: Wiley Interscience*, 1995.

[16] A. M. Y. A. Afifi, "A Radio Resource Management Framework for the 3GPP-LTE Uplink," *CU Theses*, 2012.